Measurement of the Spatial Coherence of a Soft-X-Ray Laser

J. E. Trebes, K. A. Nugent,[a] S. Mrowka, R. A. London, T. W. Barbee, M. R. Carter, J. A. Koch, B. J. MacGowan, D. L. Matthews, L. B. Da Silva, G. F. Stone, and M. D. Feit

Lawrence Livermore National Laboratory, P.O. Box 5508, Livermore, California 94450

(Received 26 April 1991)

The spatial coherence of a neonlike selenium x-ray laser operating at 206 and 210 Å has been measured using a technique based on partially coherent x-ray diffraction. The time-integrated spatial coherence of the selenium x-ray laser was determined to be equivalent to that of a quasimonochromatic spatially incoherent disk source whose diameter is comparable to the line focus of the visible-light laser pumping the x-ray laser. The spatial coherence was improved by narrowing the line focus width.

PACS numbers: 42.55.Vc, 07.85.+n, 42.25.Kb

Laboratory x-ray lasers have been available for six years as potential tools for research. Their basic characteristics such as output energy, pulse length, linewidth, and divergence have been measured. Knowledge of these characteristics has resulted in x-ray lasers being used in some preliminary application experiments including photoionization physics [1], contact microscopy of cells [2], and holography [3]. Future applications of x-ray lasers such as nonlinear x-ray optics and holographic microscopy of biological microstructures require a detailed knowledge of the spatial coherence. This paper presents the first measurement of the spatial coherence of an x-ray laser.

The spatial coherence of a quasimonochromatic light source is characterized by its mutual intensity function. This function can be frequently approximated as the product of the source intensity distribution times the source complex coherence factor (CCF) [4]. In the case of an ideal double-slit diffraction experiment, the fringe visibility as a function of slit separation is proportional to the modulus of the CCF. In fact, double-slit diffraction has been used previously to investigate the spatial coherence of extreme-ultraviolet lasers [5] and proposed for x-ray laser coherence measurements [6]. In the experiment described in this paper, the CCF is determined from the partially coherent Fresnel diffraction pattern produced by illuminating an array of slits with an x-ray laser. The diffraction pattern is recorded on film and analyzed using a generalized form of Schell's theorem valid in the Fresnel approximation [7] to obtain the time-integrated CCF of the x-ray laser. The advantage of this technique over the double-slit method is that the CCF can be obtained from a single flash exposure. A far-field version of this technique has been successfully used to determine the spatial coherence of a pulsed glass laser in a single shot using the speckle pattern produced from frosted glass [8].

In these experiments we used the Ne-like Se soft-x-ray laser produced by irradiating a thin layer of Se on a plastic foil with high-intensity (6×10^{13} W/cm^2) visible-laser light for 500 psec in a line focus geometry [9]. This results in a high-temperature, high-density plasma in which lasing occurs at 206 and 210 Å. The length and width of the x-ray laser can be varied by changing the line focus dimensions. Most of the x-ray lasers used in these experiments were 4 cm long producing 100 μJ of x-ray laser output in 200 psec. The divergence of the beam was 8 mrad FWHM in a direction perpendicular to the foil and 16 mrad FWHM parallel to it. Density gradients in the x-ray laser plasma initially refract the beam by 8 mrad horizontally away from the foil surface [10]. The hot, dense plasma also produces a broadband soft-x-ray and ultraviolet continuum which is the primary source of background in the experiment. The longitudinal coherence of the individual laser lines is 190 μm based on the measured linewidth of 15 mÅ [11]. This is significantly greater than any path-length difference in the experiment.

A uniformly redundant array [12] of slits was used as the diffracting structure in these experiments. The array consists of 27 slits spaced such that the relative spacing between any two slits occurs with the same frequency. Each spacing contributes with equal weight to the diffraction pattern and no one spacing dominates. This maximizes the signal-to-noise ratio over a wide range of spatial frequencies while still having a predictable fringe pattern. The slits are 1 mm long with widths varying from 4 to 66 μm. The minimum spacing between adjacent slits was 8 μm and the entire array was 1 mm wide, limiting measurements of the coherence functions to correlation lengths of less than 1 mm. The slit array was placed 1.156 m from the middle of the x-ray laser. At this position 0.8 mrad of the x-ray laser beam was sampled by the array. The x-ray laser was rotated 8 mrad to illuminate the array with the brightest portion of the x-ray laser beam. The use of an array of long rectangular slits results in a one-dimensional measurement of the CCF in a direction perpendicular to the slits. The slit array could be rotated about the x-ray laser axis, allowing measurements in other directions.

A multilayer x-ray mirror [13] operating at a grazing angle of 67° was placed after the slit array and used as a bandpass filter. This mirror had a calculated peak reflectivity of 30% at 208 Å and a FWHM of 17 Å. Freestanding aluminum filters ranging in thickness from 1.1 to 3.5 μm were used to block visible and ultraviolet light from reaching the detector. The combination of the mir-

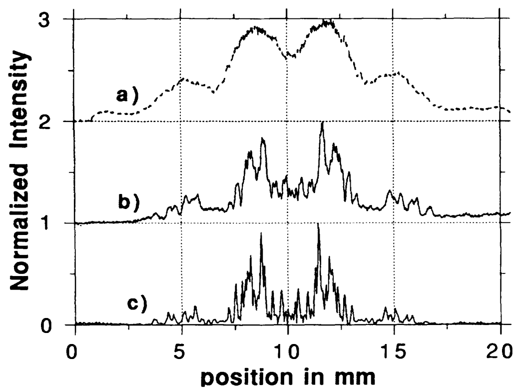

FIG. 1. Measured x-ray diffraction intensity as a function of position. (a) A 4-cm Se x-ray laser with a 300-μm-wide line focus, (b) a 4-cm Se x-ray laser with a 100-μm-wide line focus, and (c) calculated fully coherent signal.

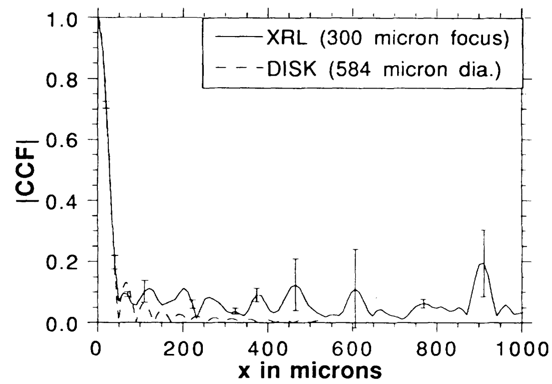

FIG. 2. The |CCF| parallel to the x-ray laser foil obtained from a 4-cm Se x-ray laser with a 300-μm line focus compared to that calculated for a 584-μm-diam spatially incoherent source.

ror and an aluminum filter reduced the background level of broadband radiation from the x-ray laser to below the threshold for detection.

The diffraction patterns were recorded on Kodak 101-07 x-ray film. The film was placed 5 m from the slit array resulting in a minimum fringe spacing of 100 μm. This is 10 times larger than the measured spatial resolution of the film [14]. The developed film was digitized and the film density was converted to linear intensity using Henke's film model [15].

The CCF of the x-ray laser was obtained numerically from the measured diffraction patterns through the use of the generalized Schell's theorem valid in the Fresnel approximation [7]. For our geometry and x-ray laser wavelength the Fraunhoffer approximation was not valid. The generalized theorem states that the diffraction pattern a distance z from the diffraction aperture is described by the convolution integral

$$I(\mathbf{r})=\int G(\mathbf{r}'/z)P(\mathbf{r}-\mathbf{r}')d\mathbf{r}',$$

where $P(\mathbf{r})$ is the Fresnel diffraction pattern of the aperture at the detector plane produced by a coherent wave described by $\Psi(\mathbf{r})$, and

$$G(\mathbf{u})=\int g(\mathbf{x})e^{-i(2\pi/\lambda)\mathbf{u}\cdot\mathbf{r}}d\mathbf{x}$$

the Fourier transform of the CCF $g(\mathbf{x})$. Given a measurement of $I(\mathbf{r})$, a knowledge of $\Psi(\mathbf{r})$, and the diffraction aperture transmission, the CCF may be recovered by deconvolution [7]. For the purposes of the data analysis, $\Psi(\mathbf{r})$ was assumed to be a spherical wave and the diffraction pattern was calculated assuming both x-ray laser wavelengths and using the measured slit-array transmission.

Coherence measurements were made with the slit-array axis both perpendicular and parallel to the x-ray laser foil and with various lengths and line focus widths. Figure 1(a) shows the measured x-ray diffraction intensity as a function position obtained with the slits perpendicular to the x-ray laser foil. This orientation measured the spatial coherence in a direction parallel to the x-ray laser foil. The x-ray laser was 4 cm long and pumped by a 300-μm-wide line focus. Figure 1(b) shows the measured diffraction pattern obtained using a 100-μm line focus. These are compared to the calculated diffraction pattern [Fig. 1(c)] obtained by assuming spatially coherent spherical waves with wavelengths of 206 and 210 Å. The measured and calculated peak locations are in good agreement.

The modulus of the CCF obtained from measured diffraction patterns as a function of relative transverse position x across the slit array is shown in Figs. 2 and 3. The |CCF| in Fig. 2 corresponds to the diffraction pattern in Fig. 1(a). Figure 3 shows the |CCF| obtained from a similar x-ray laser with the slit array oriented to measure coherence perpendicular to the foil.

Errors in the determination of the CCF result from the uncertainty in the radius of curvature of the assumed

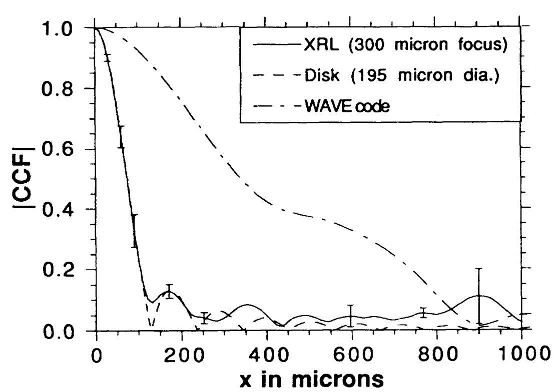

FIG. 3. The |CCF| perpendicular to the x-ray laser foil obtained from a 4-cm Se x-ray laser with a 300-μm line focus compared to that calculated for a 195-μm-diam spatially incoherent source and calculated using WAVE.

spherical wave of x-ray laser radiation. The radius was varied between 1.2 and 1.4 m in the data analysis. This distance is slightly larger than the 1.176 m distance to the far end of the x-ray laser. Values outside this range produced diffraction peak locations which noticeably disagreed with the measured locations. The error bars shown in the figures are the standard deviations produced by this variation. Nonuniformities in the film, mirror, filter, and x-ray illumination were less than 3% and would not affect the CCF significantly.

The CCF obtained from measured diffraction patterns can be compared to two theoretical models. The simplest model is to treat the x-ray laser as an amplified spontaneous emission source with a uniform, quasimonochromatic spatially incoherent source region at one end. In this case the CCF can be calculated by taking the Fourier transform of the source region. The measured |CCF| in Fig. 2 (parallel to the x-ray laser foil) is compared to the Fourier transform of a 584-μm-diam disk. The disk model and the measured coherence function are in good agreement especially in the highly coherent region at small x. In Fig. 3 the measured |CCF| (perpendicular to the foil) is compared to that calculated for a 195-μm-diam incoherent disk source. These results indicate that the time-integrated CCF can be modeled by an incoherent source ~ 200 μm in extent perpendicular to the foil surface and ~ 600 μm parallel to the foil surface. As determined by the position of the fringes in the diffraction pattern, the location of this equivalent spatially incoherent source is 2–22 cm behind the far end of the x-ray laser. The asymmetry in the source dimensions is qualitatively consistent with a Carter-Wolf quasihomogeneous source in which the low divergence should correlate with high coherence while high divergence correlates with low coherence [16]. It should be noted that while the coherence is equivalent to that of a spatially incoherent small source, the x rays are radiated into a narrow divergence beam ($\sim 1\times 10^{-4}$ sr) and not into 4π sr. The x-ray laser brightness is significantly higher than that of a disk source created in a laser plasma experiment. These coherence results disagree with the 50-μm perpendicular source size determined using an imaging spectrometer [17]. This disagreement may be explained by the fact that the spectrometer viewed the x-ray laser down the axis and not down the brightest portion of the x-ray laser beam as in the current coherence measurements.

The second model calculates the CCF using a general paraxial electromagnetic field propagation code (WAVE) [18]. This code calculates the emission, propagation, and amplification of spontaneously emitted x rays accounting for transverse variations of electron density and gain. A parabolic electron density and a quartic gain profile perpendicular to the x-ray laser foil surface were used in the calculations. The density and gain profiles were assumed to be independent of position along the x-ray laser length. These profiles are calculated [19] and are representative of the conditions at the peak of the x-ray laser pulse. The computed |CCF| perpendicular to the foil using WAVE is also shown in Fig. 3. The FWHM of the calculated degree of coherence curve is 5 times that determined from measured diffraction patterns.

The measured coherence functions disagree with the theoretical calculation and the inferred effective source size disagrees with previous measurements of the source size. A possible explanation is that the current measurements are time integrated. If the x-ray laser source size is small but moves as a function of time the effective source size would appear comparable to the extent of the motion. Simulations of the evolution of the density and gain during the x-ray laser pulse indicate that the source region may move an amount comparable to the line focus width. X-ray refraction within the x-ray laser also may be producing a larger effective source size. Although this effect is included in the WAVE calculations, errors in the assumed density and gain profiles could affect the results. This is most likely to occur early in the pulse when density gradients are the largest. The portion of the x-ray laser beam being measured occurs at this time.

Another possible explanation for the disagreement between theory and experiment is that the diagnostic and data-analysis procedures are generating incorrect coherence functions. This was checked experimentally by placing a 50-μm-wide slit at the end of the x-ray laser. We observed good agreement between the |CCF| calculated for an incoherent slit source and that measured, confirming the validity of the measurement technique.

The spatial coherence on the x-ray laser axis may be significantly better, as indicated by the small source size measured with an imaging spectrometer. The x-ray laser intensity peaks on axis later in time when the gradients in the x-ray laser plasma relax and the beam propagates along the foil axis. Transverse source motions may have a minimal effect and coherence measurements on axis could yield a 50-μm effective source size consistent with the imaging spectrometer results of Ref. [17]. On-axis experiments are planned.

The |CCF| was determined for a variety of x-ray laser operating conditions. The length of the x-ray laser was varied from 3 to 7.5 cm. This corresponds to varying the small signal gain-length product from 12 to 30. Saturation is predicted to occur at a gain-length product of approximately 15. Coherence functions similar to those described above were obtained in all cases with no significant variation as a function of laser length observed. Significant improvement in the parallel coherence was observed when the line focus width was reduced to 100 μm. The |CCF| obtained from this measurement is shown in Fig. 4 compared to the |CCF| of coherence calculated for a 94-μm-diam incoherent disk. This coherence function corresponds to a spatial coherence length [20] at the slit of 81 μm and represents a factor-of-6 improvement over

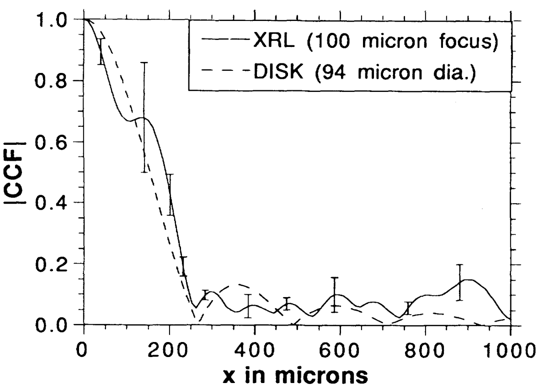

FIG. 4. The |CCF| parallel to the x-ray laser foil obtained from a 4-cm Se x-ray laser with a 100-μm line focus compared to that calculated for a 94-μm-diam spatially incoherent source.

the coherence obtained using a 300-μm-wide line focus.

In conclusion, the time-integrated complex coherence factor of a laboratory soft-x-ray laser has been determined from partially coherent diffraction patterns. The CCF was found to be equivalent to that produced by a quasimonochromatic spatially incoherent source comparable in size to the line focus width. This paves the way for experiments aimed at achieving high spatial coherence. Some improvement in the spatial coherence has already been demonstrated by reducing the transverse dimension of the x-ray laser. Future experiments using double-pass geometries with mode-selecting curved mirrors to significantly improve the spatial coherence are planned.

The authors wish to acknowledge the support of J. Kilkenny and the Nova Experiments Group and wish to thank D. Ciarlo, J. Cox, and R. Wing for their contributions. This work was performed under the auspices of the U.S. Department of Energy by Lawrence Livermore National Laboratory under Contract No. W-7405-ENG-48.

[a]Permanent address: University of Melbourne, Parkville, Victoria, Australia 3052.

[1] D. Nilsen, *et al.*, Appl. Phys. Lett. **54**, 786 (1988).
[2] C. Skinner *et al.*, J. Microsc. (Oxford) **159**, 51 (1990).
[3] J. Trebes *et al.*, Science **238**, 517 (1987).
[4] J. Goodman, *Statistical Optics* (Wiley, New York, 1985).
[5] M. Sher *et al.*, J. Opt. Soc. Am. B **8**, 114 (1991).
[6] J. Trebes *et al.*, in *Proceedings of the Conference on Short Wavelength Coherent Radiation: Generation and Applications* (Optical Society of America, Washington, DC, 1988), Vol. 2, p. 350.
[7] K. Nugent, J. Opt. Soc. Am. A **8**, 1574 (1991).
[8] A. Danilov *et al.*, Kvantovaya Elektron. (Moskow) **16**, 53 (1989) [Sov. J. Quantum Electron. **19**, 34 (1989)].
[9] D. Matthews *et al.*, Phys. Rev. Lett. **54**, 110 (1985).
[10] C. Keane *et al.*, J. Phys. B **22**, 3343 (1989).
[11] J. Koch, Lawrence Livermore National Laboratory Report (to be published).
[12] E. Fenimore and T. Cannon, Appl. Opt. **178**, 337 (1978).
[13] T. Barbee, Opt. Eng. **25**, 898 (1986).
[14] B. Henke *et al.*, J. Opt. Soc. Am. B **1**, 828 (1984).
[15] B. Henke *et al.*, J. Opt. Soc. Am. B **1**, 818 (1984).
[16] A. Marathay, *Elements of Optical Coherence Theory* (Wiley, New York, 1982).
[17] D. Whelan *et al.*, Proc. Soc. Photo Opt. Instrum. Eng. **831**, 275 (1987).
[18] M. Feit and J. Fleck, J. Opt. Soc. Am. B **7**, 2048 (1990).
[19] R. London *et al.*, J. Phys. B **22**, 3363 (1989).
[20] M. Born and E. Wolf, *Principles of Optics* (Pergamon, Oxford, 1986).